

Infrared Transition Moment Orientational Analysis (IR-TMOA) on the Structural Organization of the Distinct Molecular Subunits in Thin Layers of a High Mobility n-Type Copolymer

Supporting Information

Arthur Markus Anton,^{*,†} Robert Steyrlleuthner,^{‡,¶} Wilhelm Kossack,[†] Dieter
Neher,[‡] and Friedrich Kremer[†]

Universität Leipzig, Universität Potsdam, and Freie Universität Berlin

E-mail: anton@physik.uni-leipzig.de

*To whom correspondence should be addressed

[†]Universität Leipzig, Institut für Experimentelle Physik I, Linnéstr. 5, 04103 Leipzig, Germany

[‡]Universität Potsdam, Institut für Physik und Astronomie, Karl-Liebknecht-Str. 24 – 25, 14476 Potsdam, Germany

[¶]Freie Universität Berlin, Institut für Experimentalphysik, Arminiallee 14, 14195 Berlin, Germany

To calculate the NDI plane's normal vector, we firstly take the orthogonality of \mathbf{a} and \mathbf{b} into account, which causes the scalar product to vanish. The relative orientation of \mathbf{a} and \mathbf{b} depends on the coordinates Θ_a , Θ_b , Φ_a , and Φ_b , where the former two can be deduced from the absorbance values (Equation 3 of the Main Article), and the last two remain open. Without loss of generality we set $\Phi_b \equiv 0$ and calculate Φ_a using

$$\cos(\Phi_a) = -\frac{\cos(\Theta_a)\cos(\Theta_b)}{\sin(\Theta_a)\sin(\Theta_b)}. \quad (\text{S1})$$

Afterwards we determined the orientation of the NDI plane's normal vector as the cross product $\mathbf{a} \times \mathbf{b}$.

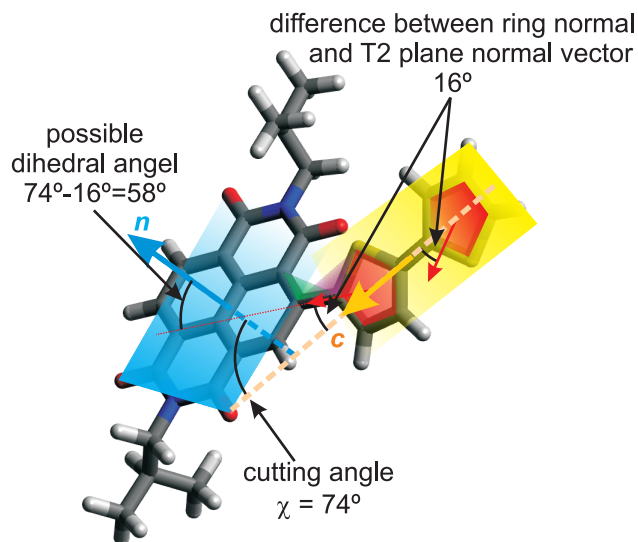


Figure S1: Schematic representation explaining how the thiophene rings' (red) torsion angle affects the difference between cutting angle χ of NDI (blue) and T2 plane (yellow) and the dihedral angle defined through atomic bonds (green and violet) between NDI unit and the *first adjacent* thiophene ring. Because the ring planes might be inclined with respect to the T2 mean plane (here $\pm 16^\circ$), the ring normal vectors deviate from the T2 plane normal vector, and hence, the dihedral angle (58°) differs by that value from the planes' cutting angle ($\chi = 74^\circ$). The twofold appearance of the value of 16° either as cutting angle χ (main text, Results part, Molecular orientation of sample CB, case 2), or as half of the torsion angle (32°) of the thiophene rings within the T2 unit is accidentally.

Table S1: Parameters of the structural model derived from the integrated absorbance depending on inclination and polarization of sample CB. The angles α , β , and γ represent Euler angles for the transition from the sample coordinate system into the principal axes system using ZXZ convention, the values A_i , A_j , and A_k denote the absorbance according to the principal axes (i, j, k) , and n represents the refractive index of the sample material. Because $\beta < 3^\circ$ and $A_i \approx A_j$, we identify the principle axis system with the sample coordinate system.

Quantity	$\nu_s(\text{C=O})$	$\nu_{as}(\text{C=O})$	$\delta(\text{C-H})$
α	43.2	133.2	44.9
β	2.7	0.4	1.5
γ	0.0	0.0	14.0
A_i	2.79	13.55	0.52
A_j	2.80	13.37	0.44
A_k	3.67	3.35	3.14
n	1.44	1.44	1.44

Table S2: Parameters of the structural model derived from the integrated absorbance depending on inclination and polarization of sample CN:Xyl notA. The angles α , β , and γ represent Euler angles for the transition from the sample coordinate system into the principal axes system using ZXZ convention, the values A_i , A_j , and A_k denote the absorbance according to the principal axes (i, j, k) , and n represents the refractive index of the sample material. Because $\beta < 3^\circ$ and $A_i \approx A_j$, we identify the principle axis system with the sample coordinate system.

Quantity	$\nu_s(\text{C=O})$	$\nu_{as}(\text{C=O})$	$\delta(\text{C-H})$
α	158.0	68.0	125.0
β	0.0	2.3	1.8
γ	0.0	2.6	0.0
A_i	1.33	5.04	0.58
A_j	1.33	4.90	0.60
A_k	1.47	2.56	0.30
n	1.44	1.44	1.44

Table S3: Parameters of the structural model derived from the integrated absorbance depending on inclination and polarization of sample CN:Xyl A. The angles α , β , and γ represent Euler angles for the transition from the sample coordinate system into the principal axes system using ZXZ convention, the values A_i , A_j , and A_k denote the absorbance according to the principal axes (i, j, k) , and n represents the refractive index of the sample material. Because $\beta < 3^\circ$ and $A_i \approx A_j$, we identify the principle axis system with the sample coordinate system.

Quantity	ν_s (C=O)	ν_{as} (C=O)	δ (C-H)
α	150.0	60.0	23.0
β	1.4	0.2	1.0
γ	0.0	2.7	162.3
A_i	1.44	5.30	0.73
A_j	1.43	5.21	0.67
A_k	1.94	2.76	0.19
n	1.44	1.44	1.44

Table S4: Geometrical orientation of the TMs \mathbf{a} , \mathbf{b} , and \mathbf{c} corresponding to ν_s (C=O), ν_{as} (C=O), and δ (C-H), and of the normal vector of the NDI plane \mathbf{n} in the framework of our model. Please note that without loss of generality we set $\Phi_{\mathbf{b}} = 0$ and calculate $\Phi_{\mathbf{a}}$ (cf. Supporting Information). Because of geometrical reasons, there exist two symmetric and exact values of $\pm\Phi_{\mathbf{a}}$, which are coequal. Consequently, the polarization of the NDI plane has also two possible values $\pm\Phi_{NDI}$ of equal rank. For simplicity we choose one possibility. The planes' cutting angle χ gives the difference/sum of the inclination of the NDI and T2 planes. The order parameters for the TMs (S_{ii}, S_{jj}, S_{kk}) are provided as well. The angles are accurate up to $\pm 5^\circ$.

Sample		\mathbf{a}	\mathbf{b}	NDI	\mathbf{c} (T2)	$\chi/^\circ$
CB	$\Theta/^\circ$	51	71	45	29	16/74
	$\Phi/^\circ$	-107	0	70	-	-
	S_{ii}	-0.05 ± 0.01	0.17 ± 0.01	-	-0.34 ± 0.01	-
	S_{jj}	-0.05 ± 0.01	0.16 ± 0.01	-	-0.31 ± 0.01	-
	S_{kk}	0.10 ± 0.01	-0.33 ± 0.01	-	0.65 ± 0.02	-
Cn:Xyl not A	$\Theta/^\circ$	53	63	49	65	16/114(66)
	$\Phi/^\circ$	-112	0	63	-	-
	S_{ii}	-0.02 ± 0.01	0.11 ± 0.01	-	0.11 ± 0.02	-
	S_{jj}	-0.02 ± 0.01	0.09 ± 0.01	-	0.13 ± 0.02	-
	S_{kk}	0.03 ± 0.01	-0.19 ± 0.01	-	-0.23 ± 0.07	-
CN:xyl A	$\Theta/^\circ$	51	63	52	70	18/122(58)
	$\Phi/^\circ$	-115	0	66	-	-
	S_{ii}	-0.05 ± 0.01	0.10 ± 0.06	-	0.19 ± 0.01	-
	S_{jj}	-0.05 ± 0.02	0.09 ± 0.02	-	0.13 ± 0.02	-
	S_{kk}	0.11 ± 0.01	-0.19 ± 0.12	-	-0.32 ± 0.05	-

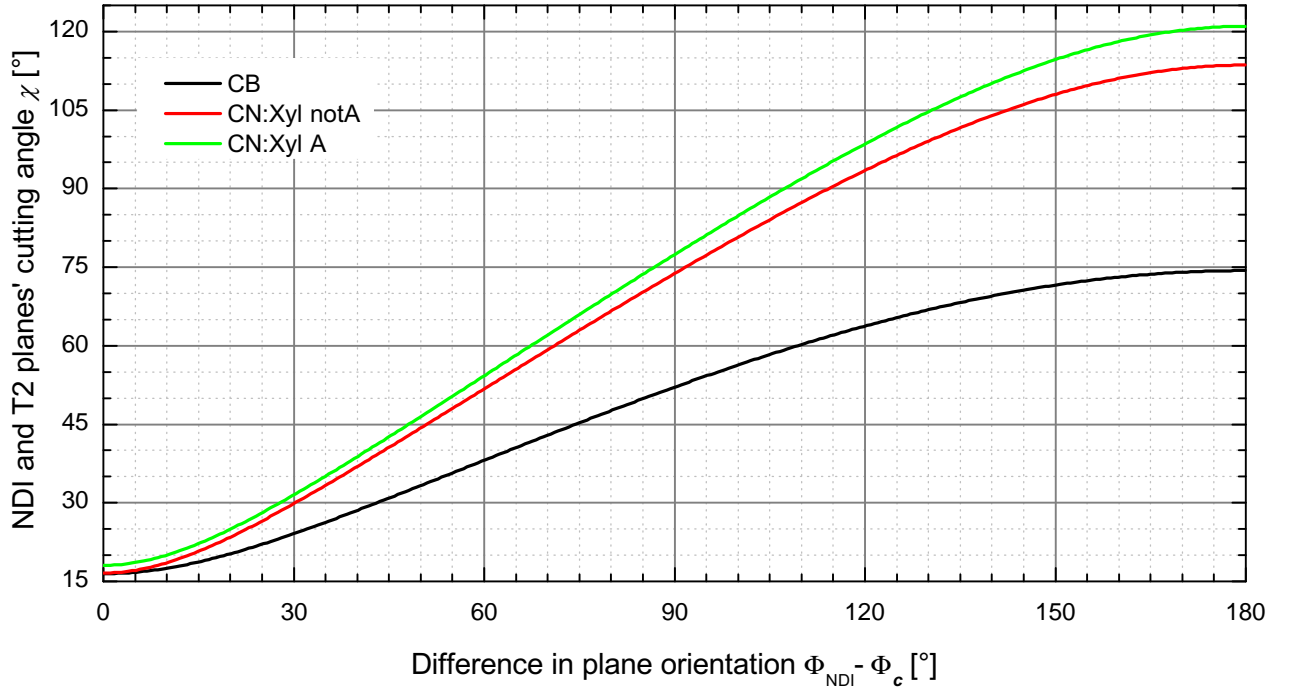


Figure S2: The planes' common cutting angle χ depending on the difference of the polarization angles of the planes' normal vectors ($\Phi_{NDI} - \Phi_c$). The values are calculated taking advantage of the experimentally derived inclination angles Θ_{NDI} and Θ_c and the scalar product of the two normal vectors ($\mathbf{n} \cdot \mathbf{c} = |\mathbf{n}| |\mathbf{c}| \cos \chi$)

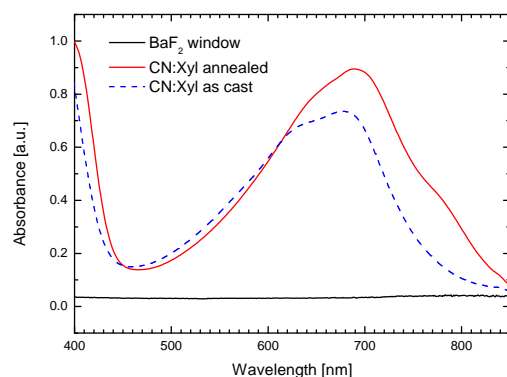


Figure S3: UV-vis absorption spectra of the samples CN:Xyl notA and CN:Xyl A. The former is dominated by aggregate I species, whereas aggregate II species is prevalent after annealing. In case of sample CB, the optical density is too high to obtain an adequate spectrum. Nevertheless, the shoulder at 790 nm indicates aggregate II species as expected (cf. Figure 2 of ref 1, respectively ref 24 in the Main Article).

References

- (1) Steyrlleuthner, R.; Di Pietro, R.; Collins, B. A.; Polzer, F.; Himmelberger, S.; Schuber, M.; Chen, Z.; Zhang, S.; Salleo, A.; Ade, H.; Facchetti, A.; Neher, D. *J. Am. Chem. Soc.* **2014**, *136*, 4245–4256